Applied Nanoscience (2022) 12:513–521
https://doi.org/10.1007/s13204-021-01705-x

ORIGINAL ARTICLE

Effect of alloying with transition metals on the aging of anomalously supersaturated solid solution of Al–Mg alloys

Tetiana O. Monastyrska[1] · Alla L. Berezina[1] · Oleh A. Molebny[1] · Andrii V. Kotko[2]

Received: 21 December 2020 / Accepted: 27 January 2021 / Published online: 13 February 2021

Abstract

The paper addresses decomposition processes of supersaturated solid solutions of Al–Mg alloys alloyed with transition metals. Al–(3.5–4)ат.%Mg–(0.25–0.5)ат.%Sc–(0.15–0.75)ат.%Zr–(0.04–0.12)ат.%Hf alloys with Sc/Zr ratios 5:2:1:0.3 have been chosen for study. The alloys were obtained by melt spinning at the quenching temperature of 1000 °C. The annealing in the temperature range of 300–450 °C was carried out to study aging processes in the alloys. Their structure and mechanical properties were examined using transmission electron microscopy (TEM), X-ray diffractometry, and hardness measurements. The temperature ranges of phase transformations were determined by measuring the temperature coefficient of resistivity $\alpha_t = 1/\rho_0 \, d\rho/dT$. It has been shown that the highest thermal stability of the alloys is achieved when the Sc/Zr ratio is equal to 1.

Keywords Al–mg alloys · Nanoparticles · Melt spinning · Anomalously supersaturated solid solution · Precipitation strengthening · Structure

Abbreviations

TEM	Transmission electron microscopy
$L1_2$	Crystal lattice structure

Introduction

The development of novel aluminum alloys that have high heat resistance and strength involves obtaining a heterogeneous structure with a large volume fraction of nano-sized particles of refractory intermetallics, which either do not interact or hardly interact with the matrix at elevated temperatures. The aging of supersaturated solid solutions of transition metals in aluminum is one of the ways to obtain such a structure. Alloys with isomorphic decomposition at high volume fractions of strengthening particles achieve high characteristics of strength and ductility. However, due to the low solubility of refractory elements in aluminum, it is not possible to obtain the volume fraction of precipitated strengthening refractory intermetallic compounds that exceeds 0.5% using conventional technologies. This stimulates the development of innovative technological processes that could significantly increase the number of refractory strengthening particles in the matrix.

In this study, the task was to achieve the precipitation of nano-scale strengthening-phase particles through the decomposition of anomalously supersaturated solid solutions obtained by rapid melt quenching (Dobatkin et al. 1995; Miroshnichenko 1982). The use of high cooling rates during the crystallization of aluminum alloys alloyed with transition metals permits light heat-resistant materials to be produced due to the increased volume fraction of the above-mentioned highly dispersed strengthening phase in the process of aging. To obtain the high volume fraction of refractory intermetallics, it is important to study the formation conditions of the anomalously supersaturated solid solutions of transition metals, along with the kinetics and morphology of phase precipitation, as well as the temperature stability of the structures obtained (Nes 1972; Nes and Billdal 1977; Nes and Ryum 1971; Ryum 1969).

In our earlier studies (Berezenia et al. 2002, 2003, 2004, 2006a, b, 2007, 2012), it was shown that the crystallization structures of rapidly quenched binary Al–Sc, Al–Zr, Al–Hf alloys, and ternary Al–Sc–Zr alloys depend on the quenching temperature of the melt. The Al–Sc and Al–Zr alloys

✉ Tetiana O. Monastyrska
tmonastyrska@gmail.com

1 G.V. Kurdyumov Institute for Metal Physics of National Academy of Sciences of Ukraine, 36, Academician Vernadsky Blvd., Kyiv-142 03680, Ukraine

2 Frantsevich Institute for Problems in Materials Science of National Academy of Sciences of Ukraine, 3, Krzhizhanovsky Str., Kyiv-142 03680, Ukraine

solidify to form an anomalously supersaturated solid solution at the quenching temperature of 1400 °C. The supersaturation of the solid solution during quenching from the melt can be increased by an order of magnitude. Fan-like structures develop at the quenching temperature of 1000 °C. The introduction of Zr into Al–Sc alloys allows one to reduce the temperature of melt quenching from 1400 to 1000 °C, resulting in the formation of the anomalously supersaturated solid solution. The decomposition of this anomalously supersaturated solid solution is continuous, with the precipitation of nano-sized spherical Al_3X (X—Sc, Zr) particles of $L1_2$-ordered phase, which is isomorphous to the matrix.

It is well known that the additional alloying of these alloys with magnesium provides an increase in the volume fraction of the strengthening phase (Driz et al. 1981; Mondolfo 1979). Our previous studies of ternary Al–Mg–Sc alloys obtained by melt spinning showed that the introduction of Mg in Al–Sc alloys allows one to obtain the anomalous supersaturated solid solution of Sc in aluminum; it is also accompanied with the inhibition of the coalescence and the loss of the Al_3Sc phase coherence during aging (Berezina et al. 2008a, b).

The formation of multicomponent intermetallic nanoscale strengthening particles is possible during the aging of multicomponent supersaturated solid solutions. The properties of alloys are determined, primarily, by the structure, morphology, and volume fraction of these particles, their surface energy, as well as the fit of crystal structures of the precipitation phase and the matrix. In our earlier study (Berezina et al. 2008a), we showed that the decomposition

Table 1 Chemical composition of alloys and parameters of ribbons

№	Concentration	Al	Mg	Sc	Zr	Hf	Mn	Cr	Ribbon sizes	
									Width *d*, мм	Thickness *t*, мкм
1	wt. %	Base	4.68	0.69	0.279	–	0.855	–	7.8	30–36
	at.%	Base	5.22	0.42	0.08	–	0.42	–		
2	wt. %	Base	4.00	0.869	0.88	–	0.803	0.407	3.3	40–60
	at.%	Base	4.51	0.53	0.26	–	0.4	0.21		
3	wt. %	Base	2.98	0.388	0.043	0.169	–	–	10	30–70
	at.%	Base	3.31	0.23	0.01	0.06	–	–		
4	wt. %	Base	4.13	0.393	0.776	0.126	–	–	7	30–60
	at.%	Base	4.60	0.24	0.23	0.04	–	–		
5	wt. %	Base	2.46	0.578	0.504	0.285	–	–	14	40–160
	at.%	Base	2.75	0.35	0.15	0.10	–	–		
6	wt. %	Base	3.45	0.596	0.515	0.312	–	–	14	40–50
	at.%	Base	3.85	0.36	0.15	0.11	–	–		
	Ат.%	осн	3.85	0.36	0.15	0.11	–	–		

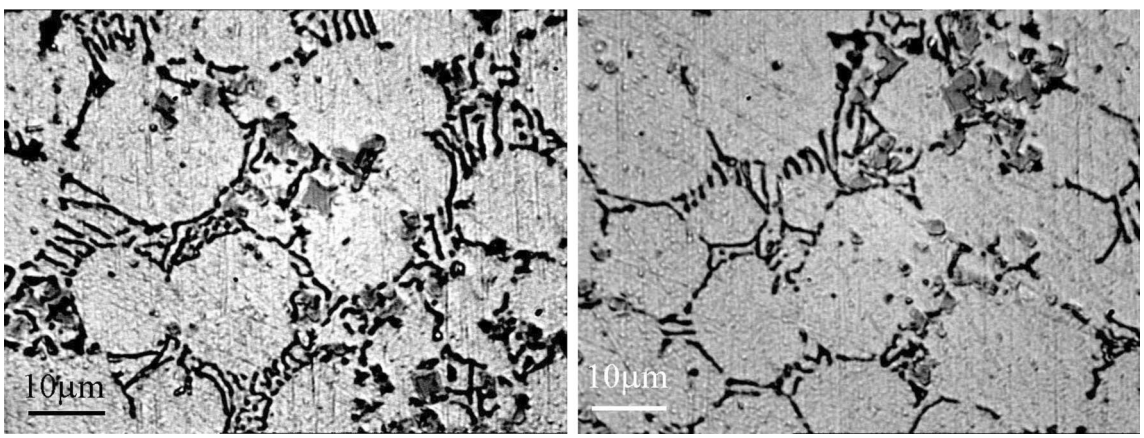

Fig. 1 Microstructure of the initial alloy obtained by crystallization at the cooling rate of 10^2 °C/s

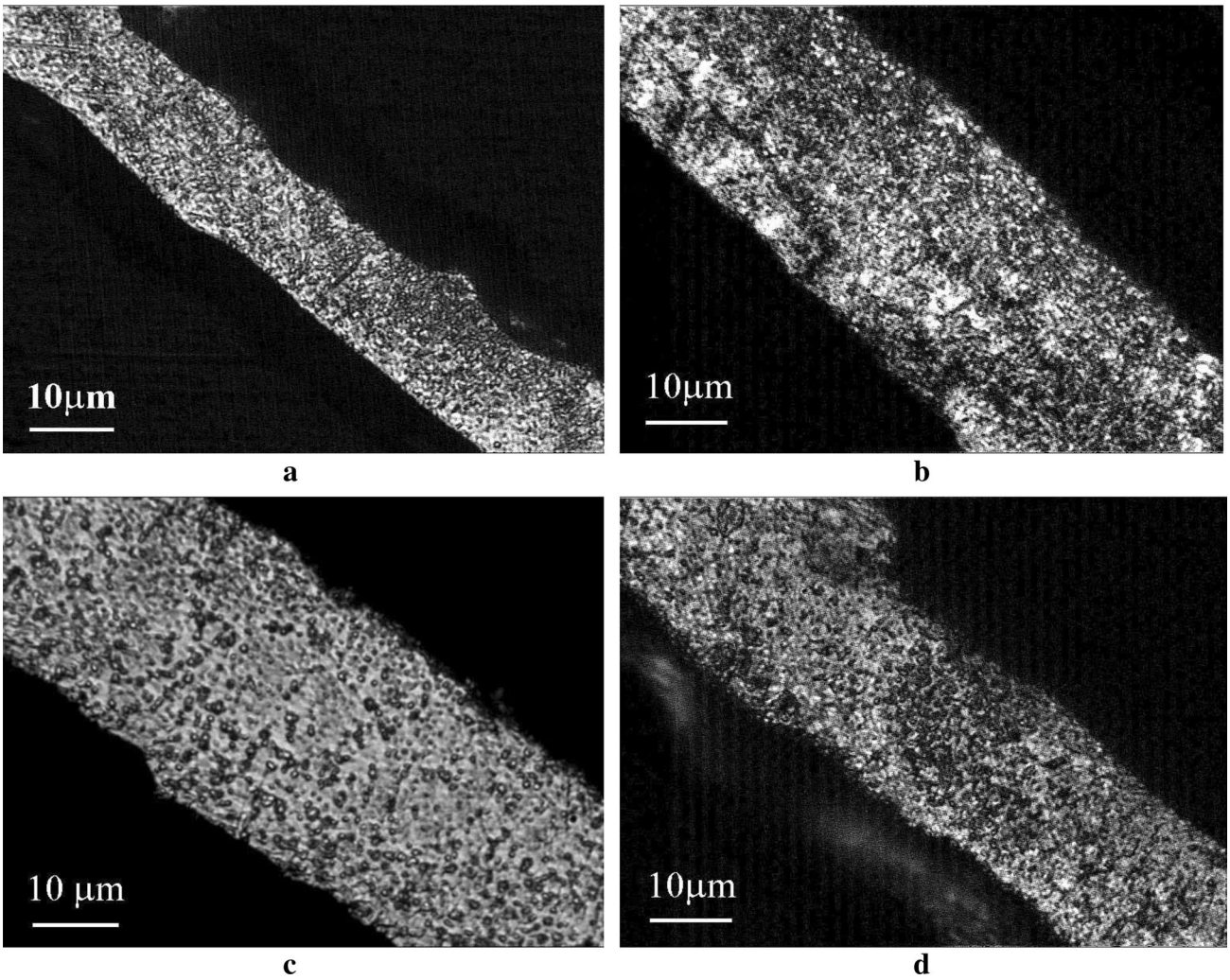

Fig. 2 Equiaxial grain structure in the cross section of rapidly quenched ribbon Nos. 1 (**a**), 4 (**b**), 5 (**c**), and 6 (**d**)

in the bulk samples of the Al–Mg–Sc–Zr–Hf alloy solidified at the cooling rate of 10^1–10^2 °C /s occurs continuously, with the precipitation of nano-composite heterophase strengthening Al_3Sc/Al_3Zr particles of the core/shell type.

The aim of the study is to obtain the anomalously supersaturated solid solution of Al–Mg–Sc–Zr–Hf rapidly quenched at the cooling rate of 10^5–10^6 °C /s and to examine the kinetics and morphology of the precipitation of nano-sized strengthening-phase particles during aging.

Experimental

In choosing the materials for research, it was taken into account that they were to provide high volume fraction and high precipitation density of the strengthening phase, as well as high thermal stability of the structure formed (Chuistov 2003). It was presumed that a high volume fraction would be provided during the decomposition of the anomalously supersaturated solid solution obtained by melt spinning. High precipitation density would result during continuous decomposition with the precipitation of particles that would have low activation energy for nucleation. Thermal stability would be ensured due to low surface energy and the low misfit parameter of the matrix with the phase formed, as well as low solubility and low diffusion coefficient of the alloying element in the matrix. The formation of the $L1_2$-ordered phase, isomorphic to the matrix, during the decomposition meets the abovementioned requirements. Therefore, the study focused on Al–Mg alloys alloyed with Sc, Zr, and Hf.

The alloys were prepared by melt spinning on a copper wheel with the rotation speed of 50 m/s by cooling from the temperature of 1080 °C. The chemical composition of the

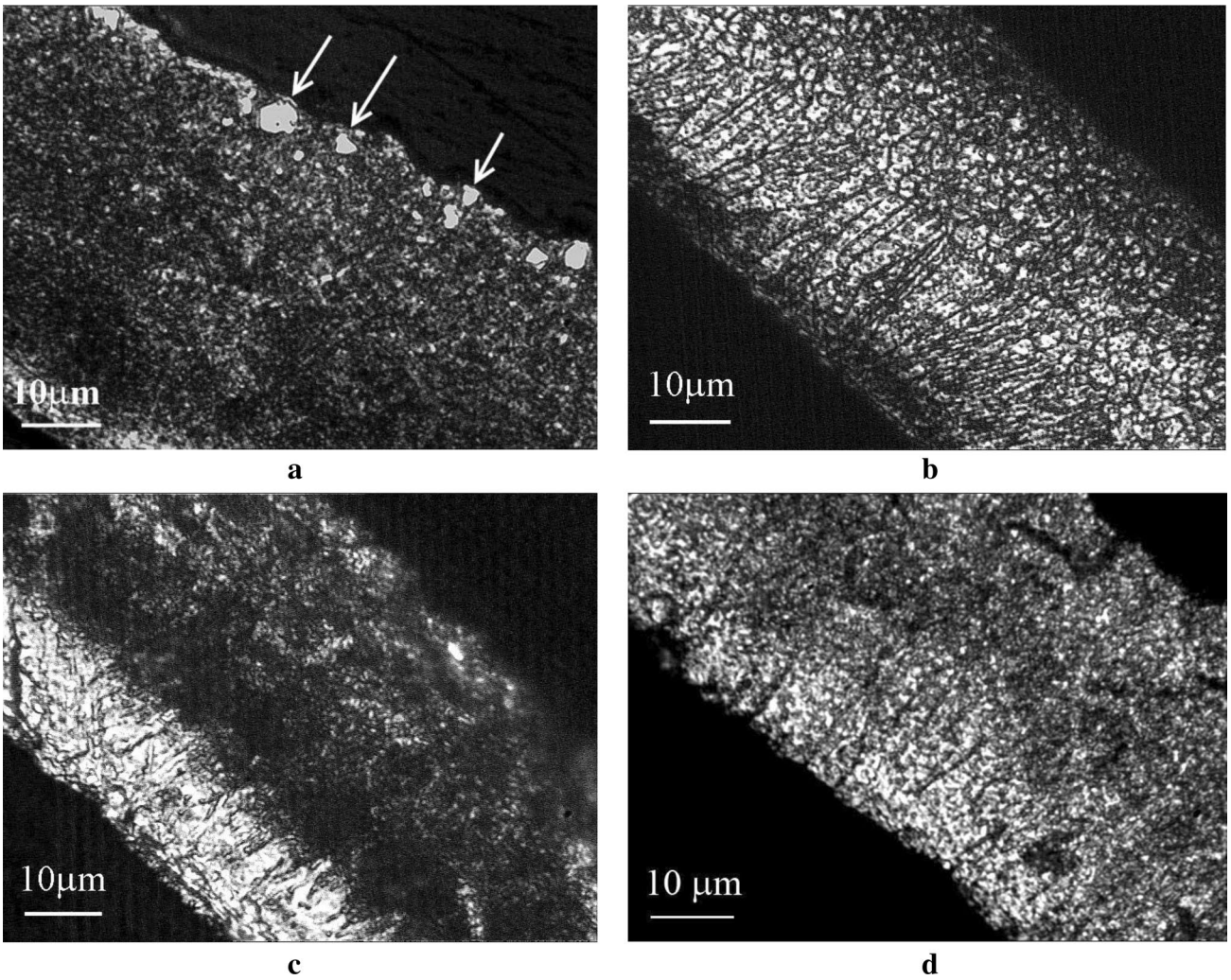

Fig. 3 Structures in the cross sections of rapidly quenched ribbon Nos. 2 (**a**), 3 (**b**), 4 (**c**), and 6 (**d**)

alloys studied, as well as the width *d* and thickness *t* of ribbons, is summarized in Table 1.

The structures of the alloys in the initial state and after aging in the temperature range of 300–450 °C were examined using transmission electron microscopy (JEM-2000FMFXII), X-ray analysis, metallography (NEOPHOT-2), and microhardness measurements. The microhardness values were measured with a PMT-3 Vickers microhardness tester using 10 g loads, the time of load duration was 12 s.

The temperature ranges of phase transformations were determined by measuring the temperature coefficient of resistivity $\alpha_t = 1/\rho_0 \cdot d\rho/dT$ during continuous heating at the rate of 3 °C/min in the temperature range of 20–500 °C. The alloys were homogenized in the atmosphere of argon, while low-temperature aging was carried out in air.

Results and discussion

Figure 1 shows the characteristic microstructures of the alloys used to produce the ribbons by the melt-spinning process. Metallographic study has shown that the alloys are crystallized, to form equiaxial grain structure with the grain size of ~ 10–20 μm. The eutectic (α-solid solution + particles of Al_3Sc phase) along the grain boundaries as well as compact equiaxial particles up to 5 μm in size and of the composition Al_3X were observed, where X is Sc, Zr, and Hf.

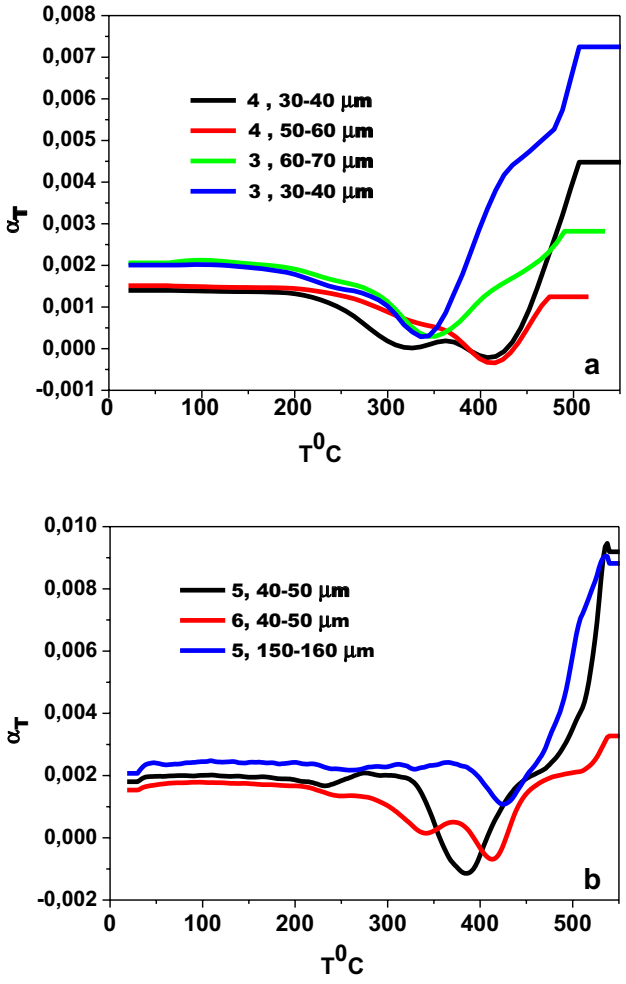

Fig. 4 Change in the temperature coefficient of electrical resistivity $\alpha_t = 1/\rho_0 \cdot d\rho/dT$ during continuous heating of alloy Nos. 3, 4 (**a**), 5, 6 (**b**) at the rate of 3 °C/min

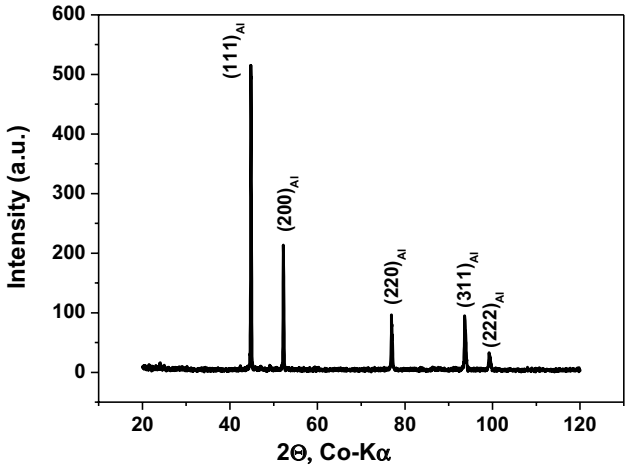

Fig. 5 X-ray diffraction pattern of the ribbons in the initial state. Co radiation

Metallographic study of the ribbons obtained by melt spinning has shown that their structures depend on the thickness of the ribbons. An equiaxial grain structure with the grain size about 1 μm is seen in the cross section when the thickness of the ribbon is less than or equal to 30 μm (Fig. 2).

If the thickness exceeds 30 μm, the microstructures of free and contact sides of the ribbons are different. A homogeneous structure with equiaxial grains is observed on the contact side adjacent to the copper wheel (the size of the zone is 25–30 μm), while a columnar structure can be seen on the free side of the ribbon (Fig. 3). The presence of large particles of $Al_6(Mn,Cr)$ intermetallic compound is observed in the cross section of ribbon No. 2 on the side of contact with the copper wheel (Fig. 3a).

The temperature intervals of the aging of the ribbons in the initial state were determined by analyzing the change in the temperature coefficient of the electrical resistivity $\alpha_t = 1/\rho_0 \cdot d\rho/dT$ during continuous heating at the rate of 3 °C/min in the temperature range of 20–500 °C (Fig. 4). The temperature coefficient of the electrical resistivity α_t when there are no phase transformations in the alloy is known to be constant. During aging, the formation of phases is accompanied with the depletion of the solid solution and the appearance of minima on the curve $\alpha_T = f(T)$, which allows us to determine the temperature ranges of the aging of supersaturated solid solutions. Due to such concentrations and heat treatment of the alloys studied, Mg remains in the solid solution. The obtained curves of changes in the temperature coefficient of electrical resistivity $\alpha_T = f(T)$ for various ribbon thicknesses are shown in Fig. 4.

As can be seen in Fig. 4, the changes in temperature coefficient of electrical resistivity (Fig. 4) during the heating of ribbon Nos. 3, 4, 5, and 6 are characterized by complex curves that correspond to different temperature ranges of aging associated with the Sc, Zr, and Hf depletion of the matrix.

The X-ray phase analysis was carried out for the ribbons in the initial state. Only the reflexes of α-solid solution were found on the X-ray diffraction pattern. An example of the X-ray diffraction pattern of the ribbons in the initial state, obtained in Co–Ka radiation, is shown in Fig. 5.

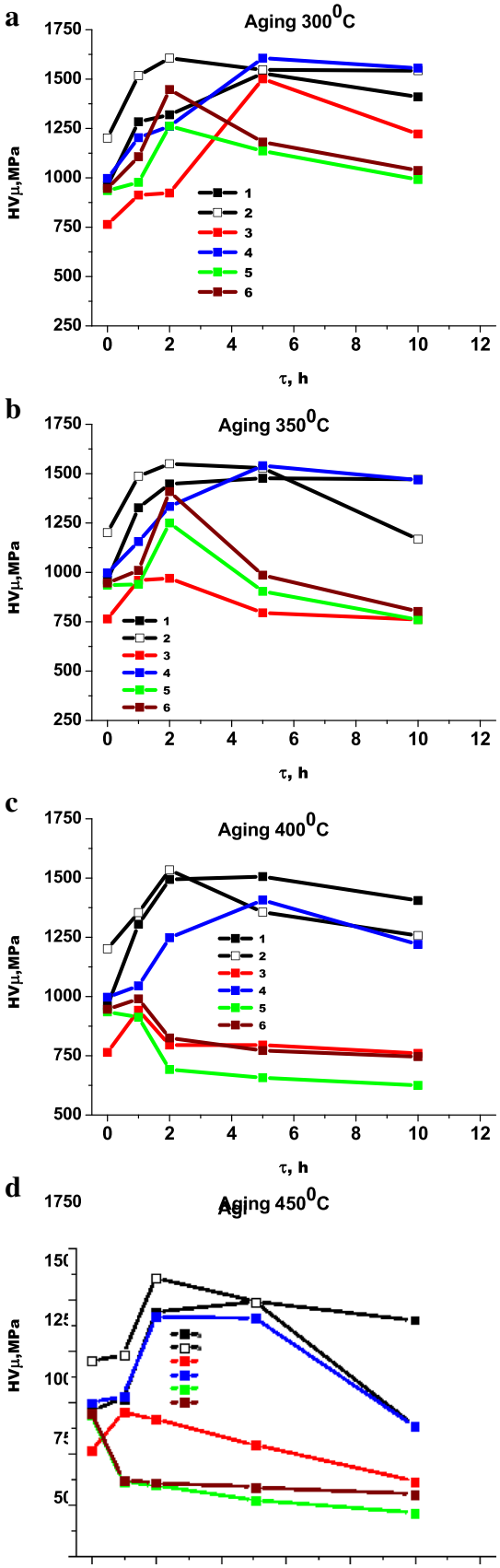

Fig. 6 Change in the microhardness of the ribbons during isothermal aging at the temperatures of 300 °C (**a**), 350 °C (**b**), 400 °C (**c**), and 450 °C (**d**)

The isothermal annealing of the ribbons at temperatures 300, 350, 400 and 450 °C for 1, 2, 5, 10, and 15 h was conducted to study aging processes. The aging of the alloys was carried out in a protective argon atmosphere. The kinetic dependences of the change in microhardness during aging at the abovementioned temperatures were determined for all ribbons. The kinetics of changes in microhardness during aging of the ribbons is presented in Fig. 6.

The largest increase in hardness (~60%) due to aging was observed for alloy Nos. 1 and 4. It should be noted that in alloy No. 4 the Zr content doubled, the concentration of Sc dropped to 0.4%, and Mn was absent. The analysis of the thermal stability of the ribbons, depending on the ratio of the scandium and zirconium content Sc/Zr in the alloy, which varied as 5:2:1:0.3, showed that the highest thermal stability of the alloy was achieved when the Sc/Zr ratio = 1 (alloy No. 4). It should be pointed out that the alloy contained neither Mn nor Cr.

The study of the effect of additional alloying of rapidly quenched Al–Mg–Sc–Zr alloy with manganese and chromium on the kinetics and the morphology of decomposition of supersaturated solid solutions has shown that the introduction of > 0.7% Mn leads to ~ 60% increase in the alloy hardness during aging. The thermal stability of the alloy grows up to 400–450 °C. Simultaneous alloying of the alloy with manganese and chromium provides additional strengthening, but its thermal stability is lower. The loss of the thermal stability of the alloy is due to the phase transformations in the primary particles of the crystallization origin, such as Al_6(Mn,Cr). The results obtained indicate that the simultaneous addition of manganese and chromium into rapidly quenched Al–Mg–Sc–Zr alloy is counterproductive.

To determine the mechanism of ribbons strengthening, TEM examinations of alloy Nos. 1, 2, 4, and 6 (Table 1) were carried out both in the initial state and after aging at 300 °C and at 450 °C for 5 h. The structures of the ribbons in the initial state and after aging are shown in Figs. 7 and 8. In the initial state, the structures of the ribbons of alloy Nos. 4 and 6 are similar, the grain size is 1–3 μm, the cells size is 0.2–0.4 μm. Low-angle grain boundaries are decorated with Al_3(Zr,Sc,Hf) primary dispersed intermetallic particles of the size ~ 0.01–0.05 μm and $L1_2$-ordered structure. Much smaller grain size (less than 0.6 μm) is observed in alloy No. 2. ~ 0.06 μm-sized particles are also observed inside

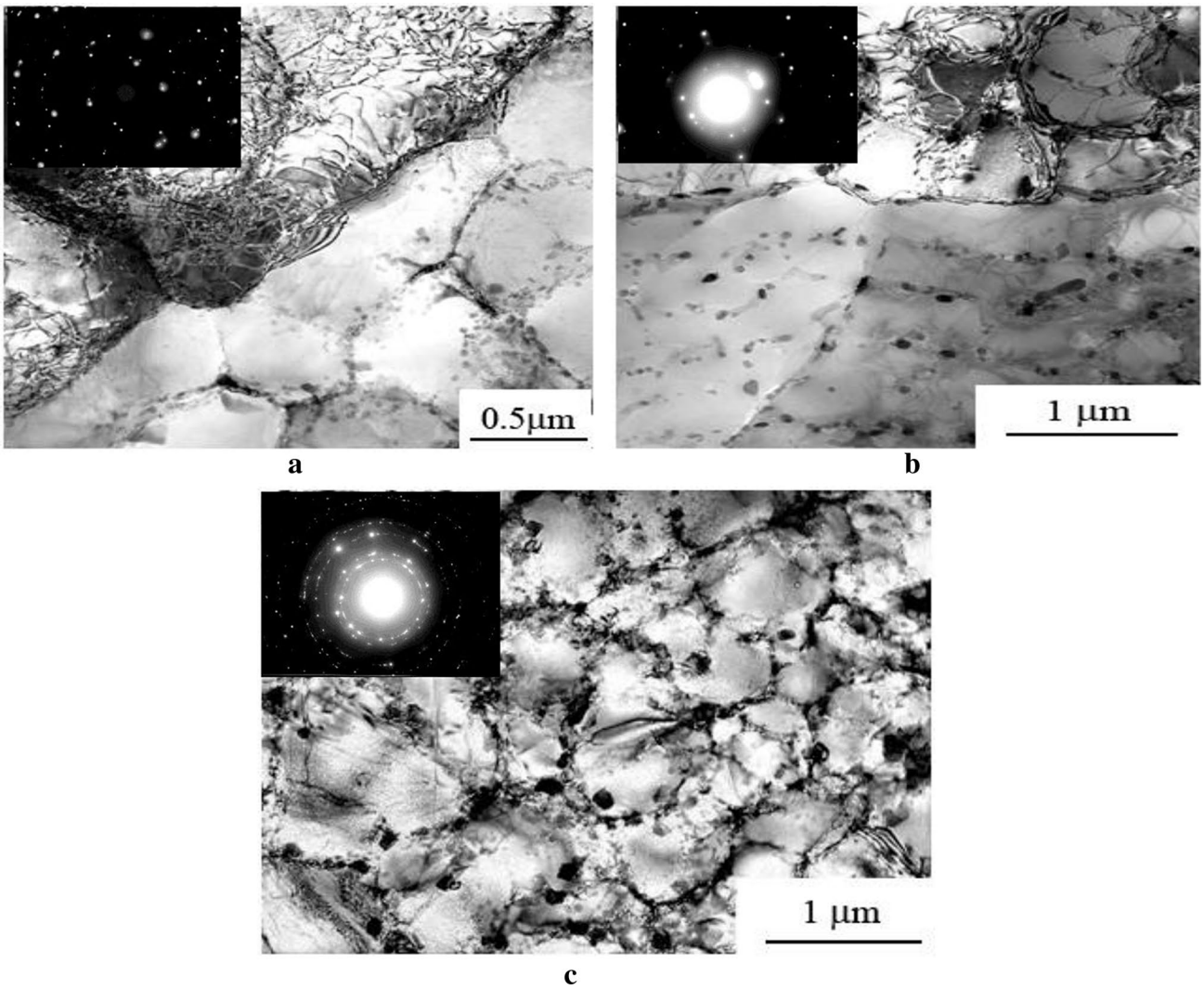

Fig. 7 Structures of ribbon Nos. 4 (**a**), 6 (**b**), and 2 (**c**) in the initial state

the grains. These could be intermetallics Al_3(Zr,Sc,Hf) of $L1_2$-ordered phase. Fine-grained precipitations are present at grain boundaries. The determination of their nature would require further research. They might be the particles of a new metastable phase containing Cr.

Strengthening in alloys occurs due to the decomposition of the supersaturated solid solution. Nano-sized particles of high-strength Al_3X (X is Sc, Zr, Hf) $L1_2$-ordered phase are formed during aging. After aging, static distortions arise in the matrix, that are accompanied by Eshby–Brown diffraction contrast on the bright-field images of the TEM studies, which indicates the precipitation of the $L1_2$-ordered phase particles isomorphic to the matrix. The structures of the ribbons after aging at 450 °C for 5 h are shown in Fig. 8. Coherent particles are observed on dark-field images; the average size d, the precipitation density Hv, and the volume fraction f of particles are presented in Table 2. Our earlier study (Berezina et al. 2008a) showed that composite Al_3Zr/Al_3Sc particles with Al_3Sc core and Al_3Zr shell are formed during high temperature aging in ternary Al–Sc–Zr alloys produced at the cooling rate of $v_{cool} = 10^2$ °C/s. The formation of Al_3Zr shell changes the nature of the interfacial fit of the particle and the matrix, it slows down the decomposition during the coalescence stage, which improves the thermal stability of the alloys. An increase in the Zr content leads to a change in the morphology and structure of the strengthening phase. Heterophase isomorphic composite particles of $L1_2/L1_2$ type are replaced by heterophase non-isomorphic ones of $D0_{23}/L1_2$ type.

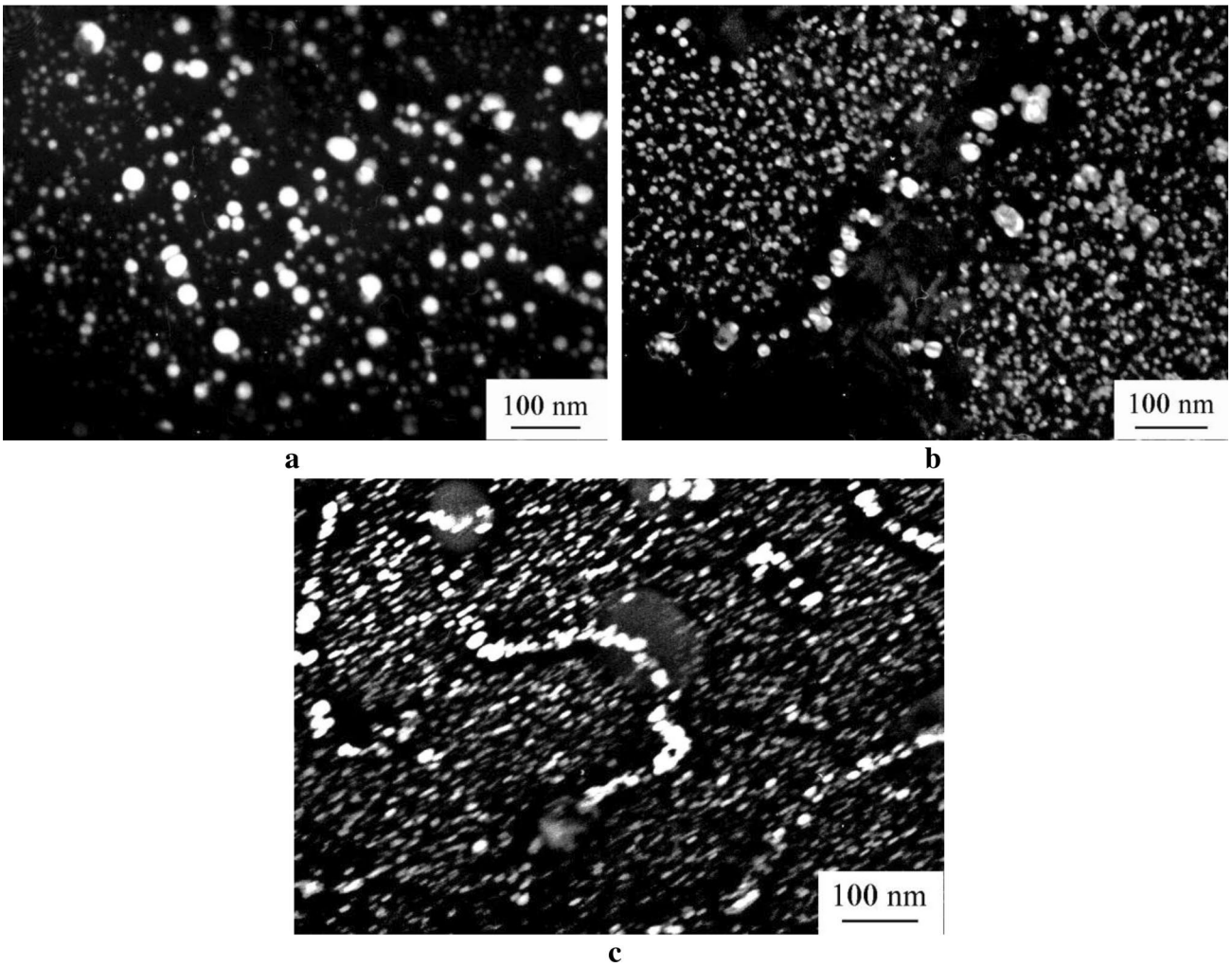

Fig. 8 The effect of Sc and Zr concentration on the morphology of the strengthening phase

Table 2 Characteristics of Al_3X phase particles after aging at 450 °C for 5 h

Alloy	*d*, nm	H_v, sm^{-3}	*f*, %
1	16	$7.3 \cdot 10^{15}$	2.5
2	15	$5.3 \cdot 10^{15}$	2.2
4	8.5	$2.2 \cdot 10^{16}$	5.8
6	9	$1.9 \cdot 10^{16}$	4.2

Conclusions

1. The multicomponent Al–(3.5–4)ат.%Mg–(0.25–0.5) ат.%Sc–(0.15–0.75)ат.%Zr–(0.04–0.12)ат.%Hf alloys are solidified, to form anomalously supersaturated solid solution with the precipitation of Al_3(Zr,Sc) primary dispersed intermetallic particles ~ 0.01–0.05 μm in size with $L1_2$-ordered structure during quenching at the cooling rate of $V \sim 10^5$–10^6 °C/c.
2. The decomposition of supersaturated solid solutions is continuous, with the formation of nano-scale particles of strengthening Al_3X (X is Sc, Zr) $L1_2$-ordered phase, which is isomorphous to the matrix.
3. The analysis of kinetic plots of the change in the hardness of alloys during aging at the temperatures of 300, 350, 400, and 450 °C, depending on the ratio of scandium and zirconium Sc/Zr content in the alloy, which varied as 5:2:1:0.3, has shown that the highest thermal stability of the alloy is achieved when the Sc/Zr ratio = 1.
4. The study of the effect of additional alloying of the rapidly quenched Al–Mg–Sc–Zr alloy with manganese and chromium on the kinetics and morphology of decomposition of supersaturated solid solutions has shown that the introduction of Mn > 0.7% leads to $a \sim 60\%$ rise in

the alloy hardness during aging. The thermal stability of the alloy increases up to 400–450 °C. Simultaneous alloying of the alloy with manganese and chromium provides additional strengthening, but the thermal stability of the alloy decreases.

Acknowledgements This work was carried out within the frame of budget project 055/16 of the G.V. Kurdyumov IMP of the N.A.S. of Ukraine.

Compliance with ethical standards

Competing interests The authors declare that they have no competing interests.

References

Berezina AL, Chuistov KV, Monastyrskaya TA, Shmidt U (2002) Structure of rapidly quenched Al-Sc alloys. Mater Technol 17(1):26–29. https://doi.org/10.1080/10667857.2002.11752960

Berezina AL, Chuistov KV, Monastyrskaya TA, Segida EA, Shmidt U, Kotko AV, Lad`yanov VI, Bel`tyukov AL, Volkov VA (2003) "Veernaya" struktura v bystrozakalennykh Al-Sc splavakh. Metallofizika i noveyshiye tekhnologii 25(12):1001–1010 ((**in Russian**))

Berezina AL, Monastyrskaya TA, Segida EA, Chuistov KV, Shmidt U, Kotko AV (2004) Phenomenon of the Anomalous Supersaturation in Al-Sc, Al-Mg-Sc Alloys Rapid Quenched from the Liquid State. Engineering Mechanics 11(5): 393–397. http://www.engineeringmechanics.cz/pdf/11_5_393.a.pdf.

Berezina AL, Budarina NN, Segida EA (2006a) Strukturnye osobennosti bystrozakalennykh alyuminievykh splavov, legirovannykh perekhodnymi metallami. Metallofizika i noveyshiye tekhnologii 28(specz. vypusk):131–138 ((**in Russian**))

Berezina AL, Segida EA, Nosenko VK, Shmidt U, Kotko AV (2006b) The effect of aging processes on the structure and properties rapidly solidified Al-Sc, Al-Zr and Al-Hf alloys. Mater Sci Forum 519–521:1815–1820. https://doi.org/10.4028/www.scientific.net/MSF.519-521.1815

Berezina AL, Segida EA, Nosenko VK, Kotko AV (2007) Obrazovanie i stabil`nost` „veernykh" struktur v bystrozakalennykh alyuminievykh splavakh, legirovannykh perekhodnymi elementami. Elektronnaya mikroskopiya i prochnost` materialov 4:57–66

Berezina AL, Monastyrskaya TA, Molebny OA, Kotko AV (2008a) Al_3Sc/Al_3Zr Composite Particles Formation in Deformed Al-Mg alloys. Aluminium Alloys: Their Physical and Mechanical Properties, Edited by Jurgen Hirsch, Birgit Skrotzki and Gunter Gottstein: 1034–103.

Berezina AL, Segida EA, Monastyrskaya TA, Kotko AV (2008b) Vliyanie skorosti kristallizaczii na anomal`noe peresyshhenie Al–Mg–Sc splavov. Metallofizika i noveyshiye tekhnologii 30(6):849–857 ((**in Russian**))

Berezina AL, Monastyrskaya TA, Molebny OA, Nosenko VK, Kotko AV (2012) Decomposition processes in the anomalous supersaturated solid solution of binary and ternary aluminium alloys alloyed with Sc and Zr. Acta Phys Pol, A 122(3):539–543. https://doi.org/10.12693/APhysPolA.122.539

Chuistov KV (2003) Starenie metallicheskikh splavov. Akademperiodika, Kiev (in Russian)

Dobatkin VI, Elagin VI, Fedorov VM (1995) Bystrozakristallizovanye alyuminievye splavy. VILS, Moskva (in Russian)

Driz ME, Pavlenko SG, Toropova LS, Bikov YuG, Ber LB (1981) O mekhanizme vliyaniya skandiya na povyshenie prochnosti i termicheskoj stabilnosti splavov sistemy Al–Mg. Doklady AN SSSR 257(2):353–356

Miroshnichenko IS (1982) Zakalka iz zhidkogo sostoyaniya. Metallurgiya, Moskva (in Russian)

Mondolfo LF (1979) Aluminium Alloys: structure and properties. Butterworths, London

Nes E (1972) Precipitation of the metastable cubic Al_3Zr-phase in subperitectic Al-Zr alloys. Acta Metall 20(4):499–506. https://doi.org/10.1016/0001-6160(72)90005-3

Nes E, Billdal H (1977) Non-equilibrium solidification of hyperperitetic Al-Zr alloys. Acta Metall 25(9):1031–1037. https://doi.org/10.1016/0001-6160(77)90132-8

Nes E, Ryum N (1971) On the formation of fan-shaped precipitates during the decomposition of a highly supersaturated Al-Zr solid solution. Scripta Metall 5(11):987–989. https://doi.org/10.1016/0036-9748(71)90142-6

Ryum N (1969) Precipitation and recrystallization in an A1–0.5 WT.% Zr-alloy. Acta Metall 17(3):269–278. https://doi.org/10.1016/0001-6160(69)90067-4